



SCUOLA INTERNAZIONALE SUPERIORE DI STUDI AVANZATI

SISSA Digital Library

A ceRNA circuitry involving the long noncoding RNA KLHL14-AS, PAX8, and BCL2 drives thyroid carcinogenesis

*Original*

A ceRNA circuitry involving the long noncoding RNA KLHL14-AS, PAX8, and BCL2 drives thyroid carcinogenesis / Credendino, S.C., Bellone, M.L., Lewin, N., Amendola, E., Sanges, R., Basu, S., Sepe, R., Decaussin-Petrucci, M., Tinto, N., Fusco, A., de Felice, M., de Vita, G.. - In: CANCER RESEARCH. - ISSN 0008-5472. - 79:22(2019), pp. 5746-5757. [10.1158/0008-5472.CAN-19-0039]

*Availability:*

This version is available at: 20.500.11767/110197 since: 2020-04-09T18:24:31Z

*Publisher:*

*Published*

DOI:10.1158/0008-5472.CAN-19-0039

*Terms of use:*

Testo definito dall'ateneo relativo alle clausole di concessione d'uso

*Publisher copyright*

note finali coverpage

(Article begins on next page)

**Title:** A ceRNA circuitry involving the long noncoding RNA Klhl14-AS, Pax8 and Bcl2 drives thyroid carcinogenesis

**Authors:** Sara C. Credendino<sup>1</sup>, Maria L. Bellone<sup>1</sup>, Nicole Lewin<sup>1</sup>, Elena Amendola<sup>1,4</sup>, Remo Sanges<sup>2</sup>, Swaraj Basu<sup>3</sup>, Romina Sepe<sup>4</sup>, Myriam Decaussin-Petrucci<sup>5</sup>, Nadia Tinto<sup>1,6</sup>, Alfredo Fusco<sup>1</sup>, Mario De Felice<sup>1,4</sup> & Gabriella De Vita<sup>1</sup>.

**Author Affiliations:** <sup>1</sup>Department of Molecular Medicine and Medical Biotechnology, University of Naples "Federico II", Naples, Italy; <sup>2</sup>Computational Genomics Laboratory, Neuroscience Area, International School for Advanced Studies (SISSA), Trieste, Italy; <sup>3</sup>Department of Medical Biochemistry and Cell Biology, Institute of Biomedicine, Sahlgrenska Academy, University of Gothenburg, Gothenburg, Sweden; <sup>4</sup>Institute of Experimental Endocrinology and Oncology "G. Salvatore", National Research Council (CNR), Naples, Italy; <sup>5</sup>Service d'Anatomie et Cytologie Pathologiques, Centre de Biologie Sud, Groupement Hospitalier Lyon Sud, Lyon, France; <sup>6</sup>CEINGE-Biotecnologie Avanzate, Naples, Italy.

**Running title:** A new lncRNA acting as ceRNA in thyroid cancer

**Abbreviations:** ceRNA (competing endogenous RNA), lncRNA (long noncoding RNA).

**Corresponding author:** Gabriella De Vita, Department of Molecular Medicine and Medical Biotechnology, University of Naples "Federico II", Via Sergio Pansini 5, 80131 Naples, Italy, phone +39 081 7463240, email gdevita@unina.it.

**Conflict of interest disclosure statement:** Authors declare that they have no competing interests.

## **Abstract**

Klhl14-AS is a long noncoding RNA expressed since early specification of thyroid bud and is the most enriched gene in the mouse thyroid primordium at E10.5. Here, we studied its involvement in thyroid carcinogenesis, by analyzing its expression in cancer tissues and different models of neoplastic transformation. Compared to normal thyroid tissue and cells, Klhl14-AS was significantly downregulated in human thyroid carcinoma tissue specimens, particularly the anaplastic histotype, thyroid cancer cell lines, and rodent models of thyroid cancer. Downregulating the expression of Klhl14-AS in normal thyroid cells decreased the expression of thyroid differentiation markers and cell death and increased cell viability. These effects were mediated by the binding of Klhl14-AS to two microRNAs, miR-182-5p and miR-20a-5p, which silenced PAX8 and BCL2, both essential players of thyroid differentiation. miR-182-5p and miR-20a-5p were upregulated in human thyroid cancer and thyroid cancer experimental models and their effects on Pax8 and Bcl2 were rescued by Klhl14-AS overexpression, confirming Klhl14-AS as a ceRNA for both PAX8 and BCL2.

This work connects deregulation of differentiation with increased proliferation and survival in thyroid neoplastic cells and highlights a novel ceRNA circuitry involving key regulators of thyroid physiology.

## **Significance**

This study describes a new ceRNA with potential tumor suppression activity and helps us better understand the regulatory mechanisms during thyroid differentiation and carcinogenesis.

## Introduction

The widest and least known part of human genome is extensively transcribed in noncoding RNA molecules, generally classified in short and long noncoding RNA based on their length. Long noncoding RNAs (lncRNAs) are broadly defined as RNA molecules longer than 200 nucleotides that appear to lack protein-coding potential (1). LncRNAs are functional molecules, acting through different mechanisms that can be generally reassumed into three types: guides, scaffolds and molecular decoys. Guides are able to target chromatin modifying complex or transcription factors to specific loci; scaffolds act as platforms to assemble protein complexes; decoys can bind to other regulatory RNAs or proteins to sequester them away to their targets (1). One abundant and well-studied class of short RNAs are microRNAs (miRNAs), 22-23 nt long RNA molecules that guide RNA-Induced Silencing Complexes (RISC) on target mRNAs and lncRNAs, to either block mRNA translation or induce target RNA decay (2,3). Several lncRNAs are able to regulate the expression of other RNAs sharing responsive elements for the same miRNA (MREs), thus acting as competitive endogenous RNA (ceRNA) (4-6). Similarly to protein-coding genes and miRNAs, lncRNAs are aberrantly expressed in cancer, thus affecting the complex regulatory circuits in which they are involved (7). The miRNA sponge activity of several lncRNAs has been shown in different kinds of cancer, including thyroid cancer, where they play either oncogenic or tumor suppressor roles (8-13).

*Klhl14-AS* is a long noncoding RNA identified as the most enriched transcript in thyroid bud at E10.5 day of mouse development (14). We recently demonstrated that it is expressed in several mouse adult tissues including thyroid (15). The expression of *Klhl14-AS* at early stages of thyroid development suggested a possible role in mechanisms regulating cell differentiation and proliferation, similarly to what described for other lncRNAs (4,16). Therefore, in this study we have investigated the expression of *Klhl14-AS* in thyroid cancer tissues and in different experimental models of thyroid neoplastic

transformation, either *in vitro* and *in vivo*, showing that this lncRNA is strongly repressed in transformed thyroid cells. We also report that *Klhl14-AS* expression is necessary for maintaining the differentiated phenotype in normal thyroid cells, likely acting as decoy for two miRNAs upregulated in thyroid cancer, targeting two important regulators of thyroid physiology, *Pax8* and *Bcl2*.

Overall, our results highlight a role of *Klhl14-AS* in the maintenance of normal thyroid phenotype, showing its contribution to the loss of differentiation and the increase of cell proliferation/survival in thyroid cancer.

## **Materials and Methods**

### **Human thyroid samples**

Human thyroid carcinoma specimens used was provided by the Service d'Anatomie et Cytologie Pathologiques, Centre de Biologie Sud, Groupement Hospitalier Lyon Sud, Pierre Bénite, France. The activity of biological samples conservation was declared under the number DC-2011-1437 to the french Ministry of Research, to the committee of people's protection of south-east IV and to the Health Regional Agency. The activity of biological material cession was agreed upon by the french Ministry of Health under the number AC-2013-1867.

### **Mice**

TetO-*BrafV600E* and *Tg-rtTA* transgenic mice were obtained from Prof JA Fagin at Sloan-Kettering Institute for Cancer Research (NY, USA), where they have been generated (17), and were crossed to obtain the double transgenic mice *Tg-rtTA*; TetO-*BrafV600E*.

Mice were maintained under pathogen-free conditions and controlled temperature, humidity, and light and were supplied with standard or implemented food and water ad libitum in the Italian Ministry-

approved (D.M. 78/213-A, and 12/2018-UT) Animal Facility of the Università Federico II, Naples, Italy. *Tg-rtTA-TetO-BrafV600E* transgenic mice were fed with a 2500 mg/kg Doxycycline supplemented fodder for one week. These studies have been approved by the Institutional Animal Care and Use Committee (IACUC) of University of Naples Federico II and by the Italian Ministry of Health with protocol n° 2013/0078506.

### **Cell culture and transfection**

HeLa, Nthy-ori 3-1, BCPAP, TPC1, 8505C, CAL62, WRO and ACT-1 cell lines were cultured in DMEM High Glucose supplemented with 10% Fetal Bovine Serum (Hyclone Thermo Fisher Scientific) and 1% pen-strep (EuroClone). FRTL-5, ERTMRASV12FRTL-5 and H-RASV12FRTL-5 were grown in Coon's modified F12 medium (EuroClone) supplemented with 5% calf serum (Hyclone Thermo Fisher Scientific) and six hormones as described (18). All cell lines used in this study were originally obtained by public cell banks (ATCC and ECACC) and frozen in large stocks before reaching 10 passages after recovery. Experiments were performed by using vials from the same passage and before reaching five passages after thawing. Cell identity was verified by DNA fingerprinting using AmpFlSTR® Identifiler®PCR Amplification Kit (Applied Biosystem). STR profiles were compared to public databases by using Cellosaurus resource at ExpASY Bioinformatics Resource Portal (<https://www.expasy.org>). Mycoplasma infection was regularly checked by Hoechst staining and observation at 500X magnification.

Tamoxifene was used at 0.4 nM to induce Ras activation. MAPK inhibitor U0126 was used at 25µM. Actinomycin D was used at 1µg/mL. Locked nucleic acid oligos (Exiqon Antisense LNA GapmeRs in vitro Standard), siRNA (ribocx life sciences siRNA duplexes bundle S) and miRNA inhibitor (Exiqon miRCURY LNA inhibitors) were transfected at 100nM, 100nM and 75nM respectively. miRNA mimics (Exiqon miRCURY LNA microRNA Mimics) were used at 5nM for endogenous gene

expression analysis and at 25nM for Luc assays. 50 ng of pCEFL-*Pax8* and -*Bcl2* or 150 ng of pCEFL-*Klhl14-AS* were used for transfections in 6-wells plates.

*Klhl14-AS* Antisense LNA GapmeRs were designed through Exiqon tool that generated the following sequences. Standard negative control is provided by the manufacturers.

*Klhl14-AS* LNA: AAGTGAGTGGAGAGGA

*KLHL14-AS* LNA: GTAAAGTGAGTCGAAA

Dicer specific siRNA was generated by ribox tool, generating a duplex with guide (see below) and passenger sequences. Standard negative control is provided by the manufacturers.

Dicer siRNA guide sequence: UUAUUCUGCAGACUUUCCCCC

All the transfections were performed using Lipofectamine 2000® (Thermo Fisher Scientific) according with manufacturer's specifications and cells were harvested at 48h, except for Actinomycin D treated cells, harvested at 24h.

### **Gene expression analyses**

Total RNA was isolated from cultured cells, mouse thyroids and human biopsies using Trizol (Sigma Aldrich) reagent and cDNA was generated with SensiFAST cDNA Synthesis Kit (BIOLINE BIO-65054), according to manufacturer's specifications. Quantitative Real-Time PCR (qRT-PCR) was performed with iTaq Universal SYBR Green Supermix (Bio-Rad) using gene specific oligos (le S1). 18S, Ciclofillin and Abelson were used as endogenous controls for detection of lncRNA and mRNAs in human, rat and mouse samples, respectively.

MiRNA-specific Reverse Transcriptase and Real-Time PCR (RT-PCR) were carried out using TaqMan® MicroRNA Reverse Transcription kit, TaqMan® (Applied Biosystems 4366596) TaqMan MicroRNA Assays (Applied Biosystems 4427975) and TaqMan® Universal PCR MasterMix, No AmpErase® UNG (Applied Biosystems 4324018) according to manufacturer's specification. *RNAU6*

was used as endogenous control for detection of miRNAs.

qRT-PCR reactions were carried out in BioRad CFX96 C1000 Touch thermal cycler. RT-PCR were performed in BioRad T100 thermal cycler, run on agarose gels and captured by BioRad CHEMIDOC XRS equipped with QuantityOne software version 4.6.5.

*In situ* hybridization analysis were performed as described (15).

### **Expression vectors**

Rat *Bcl2* CDS and mouse *Klhl14*-AS transcript isoform B (15) were amplified from FRTL-5 and mouse thyroid cDNA, respectively, using PWO SuperYield DNA polymerase (Roche 11 644 947 001) according to manufacturer's specification. Primers sequences are reported in Table S2. Both regions were then cloned in pCEFL expression vector (38121 Addgene). *Bcl2* was cloned in HindIII and XbaI sites and *Klhl14*-AS in KpnI and XbaI sites. The constructs were isolated from E.coli competent cells (Mix & Go! Competent Cells- Zymo 5a, Zymoresearch T3007) using the GenElute™ HP Plasmid Maxiprep kit (Sigma-Aldrich, NA0310). *Pax8* expression vector has been described (19).

### **Immunofluorescence assay**

Control and *Klhl14*-AS silenced-FRTL-5 were fixed and analyzed for Ki67 staining according to the following protocol:

20' in 4% paraformaldehyde, 3X 5' 1XPBS, 10' 0,5% v/v Triton-1XPBS, 3X 5' 1XPBS, 30' 0,5% W/v BSA-1XPBS, 3X 5' 1XPBS, o.n 4°C Ki67 antibody (Abcam ab16667), 3X 5' 1XPBS, 1h RT anti-rabbit antibody (Alexa Fluor, ThermoScientific A-21441), 3X 5' 1XPBS, 10' Hoechst, mounting with PBS:Glycerol. Confocal microscopy and overlay analysis were performed on a Zeiss Meta 710 Confocal Microscope with an x63 objective.

## Bioinformatic analyses

Sequences for human, mouse, rat and zebrafish, *Klhl14-AS* transcripts were taken from Ensembl v94. For zebrafish additional antisense transcripts were obtained from published studies (20,21). The region of conservation (~100 bases) overlapping the antisense transcripts was identified on the UCSC browser using Multiz alignment conservation tracks for each species as follows:

- Human

(hg38 Multiz 100way <http://hgdownload.soe.ucsc.edu/goldenPath/hg38/multiz100way/maf/>)

- Mouse

(mm10 Multiz 60way <http://hgdownload.soe.ucsc.edu/goldenPath/mm10/multiz60way/maf/>)

- Rat

(rn6 Multiz 20way <http://hgdownload.cse.ucsc.edu/goldenPath/rn6/multiz20way/rn6.20way.maf.gz>)

- Zebrafish

(zv9 Multiz8way <http://hgdownload.soe.ucsc.edu/goldenPath/danRer7/multiz8way/multiz8way.maf.gz>)

Further the conserved region was cross-verified by multiple alignment of the antisense transcripts from human, mouse, rat and zebrafish using Mafft L-INS-i (22). Prediction of miRNA target sites on the antisense transcripts and in the region of conservation was performed by Pita (23) against miRNAs sequences for each species (<ftp://mirbase.org/pub/mirbase/CURRENT/mature.fa.gz>) (24).

Predicted MREs on the *Bcl2* and *Pax8* transcripts were identified by searching for rno-miR-182 and rno-miR-20a-5p canonical (7-8-nt) and marginal (6-nt) seed-matched sites (25) using a custom Perl script.

## Luciferase reporter vectors and assays

Highly conserved region (HCR) of *Klhl14-AS* and MREs containing regions (MCR) of *Pax8* and *Bcl2* were amplified from FRTL-5 cDNA (oligos in Table S2), using PWO SuperYield DNA Polymerase (Roche 04 340 850 001) according to manufacturer's specifications. The amplified products were cloned into the pGL3 Control Vector (Promega E1751) in XbaI sites in both possible directions, with antisense sequences used as controls. All transfections were performed in HeLa cells. PRL Renilla

(Promega E2261) was used to normalize Luc activity. Protein extracts were obtained and analyzed using the Passive Lysis buffer (Promega E1941), Luciferase assay system (Promega E4550) and Renilla Luciferase assay system (Promega E2820) according manufacturer's instructions. Luciferase activity was measured by SYNERGY HT microplate reader (Biotek) equipped with software Gen5 version 2.05.

### **Cell viability**

Cell viability of control and *Klhl14-AS* LNA transfected FRTL-5 and Nthy-ori 3-1 was evaluated by Trypan Blue exclusion assay and MTS assay. 48 hours after transfection cells were stained with Trypan Blue (BioRad 1450013) following manufacturer's instructions and viable and dead cells were counted by using a manual hemacytometer. Then,  $4 \times 10^4$  FRTL-5 and  $10^4$  Nthy-ori 3-1 of both control and silenced cells were re-plated and cultured for additional 24 hours. MTS assay was performed using CellTiter96® Aqueous One Solution Cell Proliferation Assay (MTS) (Promega G3580) according to manufacturer's specifications and measured by SYNERGY HT microplate reader (Biotek) equipped with software Gen5 version 2.05.

### **RNA pull-down**

RNA pull-down was performed in FRTL-5 cells as already described (12), except that magnetic beads (Streptavidin MagneSphere Paramagnetic Particles, Promega) were saturated with 25mg of tRNA for 30' before incubation of 500µg of supernatant together with seven biotinylated DNA oligonucleotides for 2 hrs at R.T. *Klhl14-AS* oligo sequences are reported in table S3, LacZ control oligos have already been published (12).

### **Immunoblotting**

Total proteins were extracted using lysis buffer (NaCl 150mM, Tris HCl 50mM, MgCl<sub>2</sub> 5mM, Na deoxycolate 0.5 %, SDS 0.1%, Triton X-100 1%). DTT 0.1 mM, PMSF 0.5 mM, protease inhibitor cocktail (Sigma Aldrich P8340) and phosphatase inhibitor (Sigma Aldrich P0044) were freshly added to the buffer. 20µg were loaded for western blot. Immunoblots were incubated with primary antibodies: PAX8 (26) BCL2 (Santa Cruz 7382), AGO2 (Abcam ab32381), phospho-ERK (cell signaling 9101), ERK (cell signaling 9102), GAPDH (Immuno Chemical G4-C5-N) and ACTIN (A5441, Sigma-Aldrich), followed by secondary antibodies: anti-mouse (GE Healthcare NA931V) or anti-rabbit (GE Healthcare NA934V). Amersham<sup>TM</sup> ECL<sup>TM</sup> Western Blotting Detection Reagents (GE Healthcare RPN2209) were used for detection.

## Results

### ***Klhl14-AS* expression is downregulated in human thyroid cancer and experimental models of neoplastic transformation**

To investigate the involvement of *KLHL14-AS* in thyroid carcinogenesis, we analyzed its expression in twelve pairs of papillary thyroid cancer (PTC) specimens and their healthy adjacent tissue (HT), by qRT-PCR. All tumor samples were compared to all healthy ones, showing that PTCs values are characterized by a median lower with respect to that of HTs (Fig 1A). The coupling of each tumor sample with its normal counterpart, shows that *KLHL14-AS* expression is highly variable between samples, with a clear trend of reduction in eight out of twelve (67%) PTC with respect to the normal tissue (Fig. S1A). Subsequently, we analyzed nine anaplastic thyroid cancer (ATC) samples, for which healthy thyroid tissue is unavailable as ATC patients usually do not undergo surgery (27,28). Therefore, ATC tissues were compared to a pool of independent healthy thyroid samples. Figure 1B shows that *KLHL14-AS*, although at different extents, was downregulated in all ATC biopsies analyzed respect to normal thyroids.

*KLHL14-AS* levels were further investigated in cell lines of human thyroid cancers of different histotypes: BCPAP and TPC1 (PTC), WRO (follicular carcinoma), Cal62 and 8505C (ATC). *KLHL14-AS* resulted severely downregulated in all the lines analyzed, with the most pronounced decrease in ATC cell lines, Cal62 and 8505C (Fig 1C), consistently with the results obtained on ATC tissues.

These observations prompted us to explore *Klhl14-AS* regulation in experimental thyroid cancer models, both *in vitro* and *in vivo*. As *in vitro* models, we used two different cell lines obtained from FRTL-5 rat thyroid cells (29,30): ER<sup>TM</sup>-RAS<sup>V12</sup> FRTL-5 and H-RAS<sup>V12</sup>FRTL-5.

ER<sup>TM</sup>-RAS<sup>V12</sup> FRTL-5 is a tamoxifene (4OHT)-inducible system in which a chimeric RAS oncogene induces neoplastic transformation with loss of differentiation in 24 hours of 4OHT treatment (18).

*Klhl14-AS* expression was measured by qRT-PCR, revealing that the lncRNA is strongly downregulated by RAS oncogenic activation (Fig 1D).

H-RAS<sup>V12</sup>FRTL-5 is a chronically Ras-transformed cell line, showing characteristics of thyroid cancer cells (31,32). *Klhl14-AS* expression was dramatically repressed in H-RAS<sup>V12</sup> FRTL-5 with respect to parental FRTL-5 cells (Fig 1E).

*Klhl14-AS* expression *in vivo* was investigated in a mouse model of thyroid cancer where a transgenic *BrafV600E* oncogene is expressed in doxycycline (Dox)-dependent manner. *BrafV600E* activation induces poorly differentiated thyroid cancer with complete penetrance in a week of treatment (17). *Klhl14-AS* expression was analyzed by *in situ* hybridization on thyroid sections from doxycycline treated (+ Dox) and untreated (NT) mice. Neoplastic thyroids show staining for the long non-coding RNA weaker respect to the controls (Fig 1F). The downregulation of *Klhl14-AS* expression was confirmed by qRT-PCR analysis on total RNA extracted from pools of treated or untreated thyroids, confirming a dramatic decrease in neoplastic thyroids (Fig 1G). As both the *in vitro* and *in vivo* systems converge on the activation of MAPK, it is likely that such pathway could be responsible for *Klhl14-AS* down-regulation. To verify this hypothesis, we selected two human thyroid cancer cell lines, ACT-1 and Cal-62, characterized by N-RAS and KRAS mutation respectively (33). In both cell lines, the treatment with the MEK inhibitor U0126 up-regulates *Klhl14-AS* expression (Fig S1B) indicating that Ras represses the lncRNA through the activation of this pathway.

These results taken together clearly show that *KLHL14-AS* is downregulated in thyroid neoplastic transformation, regardless of the system used.

### ***Klhl14-AS* knockdown regulates thyroid cell differentiation and viability.**

In order to define the role of *Klhl14-AS* downregulation in thyroid carcinogenesis, we silenced *Klhl14-AS* expression in FRTL-5 cells by using locked nucleic acid (LNA) oligos. To obtain the

downregulation of all the *Klhl14-AS* transcript variants (15), silencing was performed with a LNA targeting a common region (Fig S2A and B). Knocked-down cells were analyzed for thyroid differentiation by qRT-PCR, revealing that *Klhl14-AS* silencing causes the decrease of the entire set of analyzed markers, although at different extents. Indeed, the expression of *Ttf1* transcription factor, Thyroperoxidase (*Tpo*) and thyroid-stimulating hormone receptor (*Tshr*) was weakly repressed while the transcription factors *Foxe1* and *Pax8* and the functional markers Thyroglobulin (*Tg*) and Sodium/Iodide Symporter (*Nis*) showed the most dramatic down-regulation (Fig 2A).

Then, to investigate the role of *Khl14-AS* in thyroid cell proliferation, we performed trypan blue exclusion assay, observing an increased percentage of viable cells upon *Klhl14-AS* down-regulation (Fig 2B). Besides, MTS assay confirmed that the lncRNA decrease causes a boost in cell metabolic activity (Fig 2C). Moreover, *Klhl14-AS*-silenced FRTL-5 cells show an increase in both *Ki67* positive nuclei (Fig 2D, E) and *Ki67* expression levels (Fig S2C) thus further suggesting the involvement of this lncRNA in the regulation of thyroid cell proliferation. To confirm these data to human thyroid cells, we knocked-down the reported human transcript in the wild type Nthy-ori 3-1 cells (Fig S2D and E), where we observed a significant reduction mainly in *FOXE1* and *PAX8* expression levels (Fig 2F). Besides, *KLHL14-AS*-silenced Nthy-ori 3-1 show an increase in cell proliferation and metabolic activity, similarly to what observed in FRTL-5 cells (Fig 2G, H).

### ***Klhl14-AS* is a miR-182-5p and miR-20a-5p target**

The ability of *Klhl14-AS* knockdown to downregulate a set of differentiation-related genes is suggestive of ceRNA role. To verify this hypothesis, we used a comparative approach to identify candidate miRNA binding sites on the *Klhl14-AS* transcript reasoning that developmentally important miRNA binding sites on the lncRNA should be conserved in vertebrates. We, therefore, aligned *KLHL14-AS* transcript models of human with that of mouse, rat and zebrafish using ClustalW,

identifying a highly conserved regions of 93 nucleotides resulting identical in the three mammalian species and sharing 85% identity with zebrafish (Fig S3A). Interestingly, this region is contained within the ultraconserved region uc.428 (34). We, then, run the PITA program with default parameters to predict miRNA binding sites on the conserved transcript fragments and took into account only those miRNAs predicted to bind on the conserved sequences in all the species. This analysis resulted in the selection of *MIR182-5p* and *MIR20a-5p* (Fig S3B and C and Table S4).

Next, we validated *Klhl14-AS* as both *Mir182-5p* and *Mir20a-5p* target, by cloning the highly conserved region (HCR) in luciferase (Luc) reporter vector in both sense and antisense orientation (*Klhl14-AS* HCR and *Klhl14-AS* HCR-AS). Reporter constructs were transfected in HeLa cells together with miR-182-5p, miR-20-5p or control miRNA mimics. Luciferase assay showed that *Klhl14-AS* HCR luminescence is reduced by both *Mir182-5p* and miR-20a-5p mimics compared to the control, while *Klhl14-AS* HCR-AS activity is only barely affected by both miRNA mimics (Fig 3A). We evaluated endogenous *Klhl14-AS* responsiveness to *Mir182-5p* and *Mir20a-5p* in FRTL-5 cells, revealing that *Klhl14-AS* was down-regulated by either *Mir182-5p* or *Mir20a-5p* overexpression, even if at different extent. Indeed, *Mir182-5p* is more efficient than *Mir20a-5p* in inducing *Klhl14-AS* down-regulation (Fig 3B).

Furthermore, we knocked-down *MIR182-5p* and *MIR20a-5p* with specific LNAs in the human PTC cell lines TPC1 and BCPAP, where they have been reported to be upregulated (35,36). In both cell lines, microRNA inhibition leads to an increase of *Klhl14-AS* levels (Fig 3C). TPC1 were also tested for viability and proliferation, showing a decrease of both parameters (Fig 3D, E).

To check if *Klhl14-AS* directly interacts with *Mir182-5p* and *Mir20a-5p*, we performed a RNA pull-down. Cytoplasmic extracts of FRTL-5 were incubated with streptavidin magnetic beads conjugated with biotinylated DNA oligonucleotides complementary to *Klhl14-AS*. Antisense LacZ oligonucleotides or no DNA conjugated beads were used as controls. Notably, *Klhl14-AS*, *Mir182-5p*,

*Mir20a-5p* and AGO2 protein were recovered, or highly enriched, only in samples obtained with *Klhl14-AS* specific oligos (Fig 3F-I). Interaction specificity was confirmed by the absence of the unrelated *Mirlet7a* in the same fraction (Fig S4). This result indicates that *Klhl14-AS* physically interacts with *Mir182-5p*, *Mir20a-5p* and AGO2, further suggesting that it might act as a decoy for these miRNAs.

### **miR-182-5p and miR-20a-5p target thyroid-relevant genes**

To search for possible genes cross-talking with *Klhl14-AS*, we looked for thyroid-specific genes among *Mir182-5p* and *Mir20a-5p* predicted targets, identifying *Pax8* as a putative target of both miRNAs. In addition *Bcl2*, another well-recognized player of thyroid differentiation and homeostasis (14,37) is predicted as miR-182-5p target (Table S5). We show that endogenous *Pax8* is down-regulated by *Mir182-5p* and *Mir20a-5p* mimics at both mRNA and protein level, thus validating *Pax8* as target of both miRNAs. At the same time, we demonstrated that *Mir182-5p* efficiently down-regulates *Bcl2*, as expected (Fig 4A, B). We then cloned for each gene the MREs-containing region (MCR), namely 3'UTR of *Pax8* and CDS of *Bcl2*, downstream to Luc reporter gene. The anti-sense sequences were used as controls. Reporter constructs were co-transfected in HeLa with either miR-182-5p or miR-20a-5p, revealing that *Pax8* MCR construct is repressed by both miRNAs (Fig 4C), and that *Bcl2* MCR is targeted by *Mir182-5p* (Fig 4D), thus confirming both genes as *Mir182-5p* targets, with *Pax8* being also targeted by *Mir20a-5p*.

### ***Klhl14-AS* acts as ceRNA for *Pax8* and *Bcl2***

We wondered if the downregulation of thyroid differentiation markers caused by *Klhl14-AS* silencing could be mediated by the above outlined miRNA-lncRNA-mRNA cross-talk.

We have already shown that *Pax8*, together with the other thyroid differentiation genes, are

dramatically downregulated in ER<sup>TM</sup>-RAS<sup>V12</sup> FRTL-5 and H-RAS<sup>V12</sup>FRTL-5 (18). *Pax8* has also been shown to be repressed in the BrafV600E-driven thyroid cancer mouse model (17) and in most human thyroid cancer cell lines (38-41). Nevertheless, these data were independently confirmed by a new set of experiments (Fig S5 A-D).

The expression of *Bcl2* was measured in our thyroid cancer models, observing that it is severely downregulated *in vitro*, in ER<sup>TM</sup>-RAS<sup>V12</sup> FRTL-5, in H-RAS<sup>V12</sup> FRTL-5 (Fig 5A,B) *in vivo*, in doxycycline-dependent BrafV600E-induced thyroid cancer (Fig 5C) and in human thyroid cancer cell lines, (Fig 5D), thus showing that it follows the same trend as *Klhl14-AS* and *Pax8*.

We have shown that *Klhl14-AS* downregulation strongly represses *Pax8* expression (Fig 2B). Silencing the lncRNA in FRTL-5 and Nthy-ori 3-1 cells resulted in dramatic repression of *Bcl2* levels as well (Fig 5E).

To verify if *Pax8* and *Bcl2* downregulation induced by lncRNA knockdown requires the presence of miRNAs, we performed *Klhl14-AS* silencing together with *Dicer* silencing, observing that *Pax8* and *Bcl2* levels resulted de-repressed by *Dicer* knocking-down (Fig 5F).

Moreover, we tested the ability of *Klhl14-AS* to acts as miRNA decoy by overexpressing the lncRNA in the presence of *Mir182-5p* and *Mir20a-5p* mimicks, showing that *Pax8* and *Bcl2* expression are rescued by *Klhl14-AS* overexpression (Fig 5G).

As ceRNA mechanisms act at post-transcriptional level, we tested the effects of *Klhl14-AS* knockdown in the presence of Actinomycin D (Acto-D). Figure 5G shows that though Acto-D treatment represses the expression of all the genes analyzed, the knockdown of *Klhl14-AS* is still able to exert an inhibitory effect (Fig 5H). These results taken together strongly suggest that this lncRNA acts through a post-transcriptional and miRNA-mediated decoy mechanism.

To explore if *Pax8* and *Bcl2* play a role in the generalized loss of differentiation caused by *Klhl14-AS* down-regulation, we re-expressed their CDS in lncRNA-silenced FRTL-5 (Fig S6A), revealing that

both *Pax8* and *Bcl2* rescue the expression of all differentiation markers reduced by *Klhl14-AS* silencing, including endogenous *Pax8* and *Bcl2* (Fig 5I). Differentiation markers expression was not increased by *Pax8* or *Bcl2* overexpression in the presence of control LNA (Fig S6B).

### **Klhl14-AS, PAX8 and BCL2 correlation in human thyroid cancer**

RNAs acting as ceRNA usually show similar trends of expression. We have shown that this is the case for *Klhl14-AS*, *PAX8* and *BCL2* in experimental cancer models. Thus we investigated such issue in human thyroid cancer samples. *PAX8* and *BCL2* resulted invariably down-regulated in all ATC samples analyzed (Fig 6A). Conversely, in PTC samples we observed a larger range of values of *PAX8* expression with a median lower in PTC than normal thyroids (Fig 6B), while *BCL2* shows a more homogeneous trend with a clear reduction of its median in PTC compared to healthy thyroids (Fig 6C). By combining these data with those already obtained for *Klhl14-AS* (Fig. 1A) it is worth noting that both *PAX8* and *BCL2* show a positive correlation with the lncRNA (Fig 6D,E) in the analyzed PTC samples.

To confirm these data on a wider set of samples, we interrogated the GEPIA database (<http://gepia.cancer-pku.cn/index.html> <https://academic.oup.com/nar/article/45/W1/W98/3605636>), for differential expression of *PAX8*, *BCL2* and *KLHL14-AS* between normal and neoplastic thyroid tissues, observing that all three genes are downregulated in thyroid cancer (Fig S7).

Therefore, *PAX8*, *BCL2* and *KLHL14-AS* show a similar behaviour in all the thyroid cancer models analyzed and in a large number of human thyroid carcinomas, as expected accordingly to ceRNA hypothesis.

### **miR-182-5p and miR-20a-5p are upregulated in thyroid cancer**

We asked at what extent the outlined ceRNA circuit is actually operating in thyroid cancer. Notably,

both *MIR182-5p* and *MIR20a-5p* have been reported to be upregulated in thyroid cancer (35,36,42). To confirm this trend in our samples, we measured *MIR182-5p* and *MIR20a-5p* expression in seven of the PTC biopsies already analyzed for *KLHL14-AS* expression, observing that both miRNAs are increased in cancer with respect to the normal tissue (Fig 7A, B). Both miRNAs resulted up-regulated also in all the six ATC samples analyzed, (Fig 7C) and in human thyroid cancer cell lines (Fig 7D).

Subsequently, we evaluated *Mir182-5p* and *Mir20a-5p* expression in the neoplastic-transformation models. Both miRNAs resulted up-regulated by RAS chronic activation in H-RAS<sup>V12</sup>FRTL-5 (Fig 7E). They also show a dramatic increase in doxycycline-induced *BrafV600E*-dependent thyroid cancer in mouse (Fig 7F).

Therefore, these results clearly demonstrate that the expression of *MIR182-5p* and *MIR20a-5p* in cancer shows an opposite regulation with respect to that of *KLHL14-AS*, *PAX8* AND *BCL2*, strongly suggesting that *MIR182-5p* and *MIR20a-5p* could play a role in the downregulation of the three genes in thyroid cancer, likely mediating a ceRNA circuitry.

In conclusion, our data taken together indicate a cross-talk between *KLHL14-AS* and *PAX8/BCL2* mediated by *MIR182-5p* and *MIR20a-5p* in normal as well as in transformed thyroid cells.

## Discussion

The differentiation status of neoplastic cells is a general measure of tumor malignancy, being lost in the most advanced and aggressive form of most cancer types. In thyroid cancer, the presence of differentiated cells is even more important, as their unique ability of capturing iodine can be used to treat patients with radioiodide after surgery, to eradicate residual and/or metastatic cancer cells. Poorly differentiated and anaplastic thyroid cancers lack this differentiated function and hence radioiodide treatment is not effective (43). Here we describe for the first time the role of a long noncoding RNA, named *Klh14-AS*, in thyroid differentiation, showing that such lncRNA is necessary for the

maintenance of a fully differentiated state of cultured thyroid cells. By using multiple experimental tools, we show that *KLHL14-AS* is drastically repressed in human thyroid cancer biopsies and cell lines, and shows a similar behaviour in experimental models of thyroid transformation, regardless the species and the system used, *in vivo* or *in vitro*. This univocal behavior is indicative of the robustness of such data.

There are several lncRNA playing key roles in the regulation of cell differentiation, well described for myogenesis, and for other cell types (44,45). One of the most frequent mechanisms of lncRNAs action in differentiation-related circuits is to act as decoys for miRNAs targeting master regulators of gene expression programs. This appears to be the case also for *Klhl14-AS*, that we show to compete with *Pax8*, an essential regulator of thyroid differentiation, for the binding to *Mir182-5p* and *Mir20a-5p* and with *Bcl2*, a survival factor essential in thyroid development (14,37) for the binding to *Mir182-5p*.

Thyroid neoplastic rodent models *in vitro* and *in vivo* revealed that *Klhl14-AS* is severely down-regulated in carcinogenesis. These data, together with *KLHL14-AS* repression more homogeneous and dramatic in ATC than in PTC samples, strongly suggest that the loss of this lncRNA is strictly related to the differentiation state. This has been confirmed in rat and human wild type cultured thyroid cells, in which differentiation markers decrease upon the lncRNA inhibition, indicating that *KLHL14-AS* down-regulation could be one of the primary events rather than a consequence of thyroid neoplastic transformation. Moreover, knocking-down of *Klhl14-AS* also induces an increase in cell viability and proliferation, two crucial events in cancer development, thus supporting a tumor-suppressor role for this lncRNA.

*MIR182-5p* and *MIR20a-5p* have been already reported to be up-regulated in thyroid cancer (35,36,42), with our data confirming this trend in human samples and in experimental models. We show that both miRNAs are increased upon thyroid transformation thus showing an inverse correlation with the lncRNA. Besides, this up-regulation is more evident in ATC than in PTC biopsies, indicating that

*MIR182-5p* and *MIR20a-5p* increase is related to advanced and less differentiated cancers. It is noteworthy that inhibition of both miRNAs increase the endogenous lncRNA levels in papillary thyroid cancer cell lines, supporting our hypothesis that *KLHL14-AS* down-regulation in thyroid cancer is mediated by *MIR182-5p* and *MIR20a-5p*. In addition, the physical interaction observed between *Klhl14-AS*, AGO2 and both miRNAs indicates that *Klhl14-AS* acts as decoy for *Mir182-5p* and *Mir20a-5p*. This is confirmed by the ability of *Klhl14-AS* to rescue *Pax8* and *Bcl2* repression exerted by the two miRNAs.

Notably, here we demonstrate that two thyroid-relevant genes, *Pax8* and *Bcl2*, are *Mir182-5p* targets, and that *Pax8* is also targeted by *Mir20a-5p*. Further, mRNAs of both *PAX8* and *BCL2* show a positive correlation with *KLHL14-AS* in human thyroid cancers. Accordingly, *PAX8* has already been reported as candidate target of *Mir182-5p* and *Mir20a-5p* (46), while *BCL2* has been validated as *Mir182-5p* target in prostate cancer (47). We show that the effects of *Klhl14-AS* on differentiation are miRNA-mediated and exerted at post-transcriptional level, with *Pax8* and *Bcl2* being the main targets. Indeed, re-expression of either *Pax8* or *Bcl2* rescues differentiation markers expression, in particular of *Nis*, thus corroborating the proposed mechanism .

These evidences allow us to propose that a ceRNA network involving *KLHL14-AS*, *PAX8* and *BCL2* acts in normal cells by buffering the expression of essential cell regulators, being instead deranged in thyroid carcinogenesis. Moreover, we observed that the interaction between these three genes and *MIR182-5p* and *MIR20a-5p* is conserved in human, mouse and rat models, highlighting that it could represent a very relevant mechanism supporting thyroid cancer onset and development. Both miRNAs target indeed an ultraconserved sequence of the lncRNA, found identical in the three species and highly conserved also in zebrafish, suggesting that such network is under a strong positive selection.

In conclusion, our work sheds light on new players and networks involved in thyroid differentiation and carcinogenesis. Moreover, further studies should investigate the prognostic value of *KLHL14-AS*

and/or *MIR182-5p* and *MIR-20A-5p* as novel thyroid carcinoma biomarkers. Finally, it would be interesting to evaluate if the inhibition of their crosstalk may be exploited as a new therapeutic approach in fighting the most advanced forms of thyroid carcinoma.

## Acknowledgements

We thank Prof. Roberto Di Lauro for helpful discussions, Prof. James A. Fagin for providing the tetO-Braf mouse model and Mr. Luigi Di Guida for technical assistance with mice handling. This work was supported by the Italian Ministry of University and Research (MIUR) grant PON03PE\_00060\_7 and by POR Campania FESR 2014-2020 "SATIN" grant, both to GDV.

## References

1. Marchese FP, Huarte M. Long non-coding RNAs and chromatin modifiers: their place in the epigenetic code. *Epigenetics* **2014**;9:21-6
2. Gregory RI, Chendrimada TP, Cooch N, Shiekhattar R. Human RISC couples microRNA biogenesis and posttranscriptional gene silencing. *Cell* **2005**;123:631-40
3. Wu L, Fan J, Belasco JG. MicroRNAs direct rapid deadenylation of mRNA. *Proceedings of the National Academy of Sciences of the United States of America* **2006**;103:4034-9
4. Cesana M, Cacchiarelli D, Legnini I, Santini T, Sthandier O, Chinappi M, *et al.* A long noncoding RNA controls muscle differentiation by functioning as a competing endogenous RNA. *Cell* **2011**;147:358-69
5. Wang KC, Chang HY. Molecular mechanisms of long noncoding RNAs. *Molecular cell* **2011**;43:904-14
6. Salmena L, Poliseno L, Tay Y, Kats L, Pandolfi PP. A ceRNA hypothesis: the Rosetta Stone of a hidden RNA language? *Cell* **2011**;146:353-8
7. Huarte M. The emerging role of lncRNAs in cancer. *Nat Med* **2015**;21:1253-61
8. Yoon H, He H, Nagy R, Davuluri R, Suster S, Schoenberg D, *et al.* Identification of a novel noncoding RNA gene, NAMA, that is downregulated in papillary thyroid carcinoma with BRAF mutation and associated with growth arrest. *International journal of cancer* **2007**;121:767-75
9. Jendrzewski J, He H, Radomska HS, Li W, Tomsic J, Liyanarachchi S, *et al.* The polymorphism rs944289 predisposes to papillary thyroid carcinoma through a large intergenic noncoding RNA gene of tumor suppressor type. *Proceedings of the National Academy of Sciences of the United States of America* **2012**;109:8646-51
10. Xia B, Hou Y, Chen H, Yang S, Liu T, Lin M, *et al.* Long non-coding RNA ZFAS1 interacts with miR-150-5p to regulate Sp1 expression and ovarian cancer cell malignancy. *Oncotarget* **2017**;8:19534-46
11. Laneve P, Po A, Favia A, Legnini I, Alfano V, Rea J, *et al.* The long noncoding RNA linc-NeD125 controls the expression of medulloblastoma driver genes by microRNA sponge

- activity. *Oncotarget* **2017**;8:31003-15
12. Mangiavacchi A, Sorci M, Masciarelli S, Larivera S, Legnini I, Iosue I, *et al.* The miR-223 host non-coding transcript linc-223 induces IRF4 expression in acute myeloid leukemia by acting as a competing endogenous RNA. *Oncotarget* **2016**;7:60155-68
  13. Kim D, Lee WK, Jeong S, Seol MY, Kim H, Kim KS, *et al.* Upregulation of long noncoding RNA LOC100507661 promotes tumor aggressiveness in thyroid cancer. *Molecular and cellular endocrinology* **2016**;431:36-45
  14. Fagman H, Amendola E, Parrillo L, Zoppoli P, Marotta P, Scarfo M, *et al.* Gene expression profiling at early organogenesis reveals both common and diverse mechanisms in foregut patterning. *Developmental biology* **2011**;359:163-75
  15. Credendino SC, Lewin N, de Oliveira M, Basu S, D'Andrea B, Amendola E, *et al.* Tissue- and Cell Type-Specific Expression of the Long Noncoding RNA Klhl14-AS in Mouse. *International journal of genomics* **2017**;2017:9769171
  16. Twayana S, Legnini I, Cesana M, Cacchiarelli D, Morlando M, Bozzoni I. Biogenesis and function of non-coding RNAs in muscle differentiation and in Duchenne muscular dystrophy. *Biochemical Society transactions* **2013**;41:844-9
  17. Chakravarty D, Santos E, Ryder M, Knauf JA, Liao XH, West BL, *et al.* Small-molecule MAPK inhibitors restore radioiodine incorporation in mouse thyroid cancers with conditional BRAF activation. *The Journal of clinical investigation* **2011**;121:4700-11
  18. De Vita G, Bauer L, da Costa VM, De Felice M, Baratta MG, De Menna M, *et al.* Dose-dependent inhibition of thyroid differentiation by RAS oncogenes. *Mol Endocrinol* **2005**;19:76-89
  19. D'Andrea B, Iacone R, Di Palma T, Nitsch R, Baratta MG, Nitsch L, *et al.* Functional inactivation of the transcription factor Pax8 through oligomerization chain reaction. *Mol Endocrinol* **2006**;20:1810-24
  20. Pauli A, Valen E, Lin MF, Garber M, Vastenhouw NL, Levin JZ, *et al.* Systematic identification of long noncoding RNAs expressed during zebrafish embryogenesis. *Genome research* **2012**;22:577-91
  21. Ulitsky I, Shkumatava A, Jan CH, Sive H, Bartel DP. Conserved function of lincRNAs in vertebrate embryonic development despite rapid sequence evolution. *Cell* **2011**;147:1537-50
  22. Katoh K, Kuma K, Toh H, Miyata T. MAFFT version 5: improvement in accuracy of multiple sequence alignment. *Nucleic acids research* **2005**;33:511-8
  23. Kertesz M, Iovino N, Unnerstall U, Gaul U, Segal E. The role of site accessibility in microRNA target recognition. *Nature genetics* **2007**;39:1278-84
  24. Griffiths-Jones S, Saini HK, van Dongen S, Enright AJ. miRBase: tools for microRNA genomics. *Nucleic acids research* **2008**;36:D154-8
  25. Bartel DP. MicroRNAs: target recognition and regulatory functions. *Cell* **2009**;136:215-33
  26. Francis-Lang H, Zannini M, De Felice M, Berlingieri MT, Fusco A, Di Lauro R. Multiple mechanisms of interference between transformation and differentiation in thyroid cells. *Molecular and cellular biology* **1992**;12:5793-800
  27. Ragazzi M, Ciarrocchi A, Sancisi V, Gandolfi G, Bisagni A, Piana S. Update on anaplastic thyroid carcinoma: morphological, molecular, and genetic features of the most aggressive thyroid cancer. *International journal of endocrinology* **2014**;2014:790834
  28. Saini S, Tulla K, Maker AV, Burman KD, Prabhakar BS. Therapeutic advances in anaplastic thyroid cancer: a current perspective. *Molecular cancer* **2018**;17:154
  29. Berlingieri MT, Portella G, Grieco M, Santoro M, Fusco A. Cooperation between the polyomavirus middle-T-antigen gene and the human c-myc oncogene in a rat thyroid epithelial differentiated cell line: model of in vitro progression. *Molecular and cellular biology*

- 1988**;8:2261-6
30. Fusco A, Berlingieri MT, Di Fiore PP, Portella G, Grieco M, Vecchio G. One- and two-step transformations of rat thyroid epithelial cells by retroviral oncogenes. *Molecular and cellular biology* **1987**;7:3365-70
  31. De Menna M, D'Amato V, Ferraro A, Fusco A, Di Lauro R, Garbi C, *et al.* Wnt4 inhibits cell motility induced by oncogenic Ras. *Oncogene* **2013**;32:4110-9
  32. Frezzetti D, De Menna M, Zoppoli P, Guerra C, Ferraro A, Bello AM, *et al.* Upregulation of miR-21 by Ras in vivo and its role in tumor growth. *Oncogene* **2011**;30:275-86
  33. Leboeuf R, Baumgartner JE, Benezra M, Malaguarnera R, Solit D, Pratilas CA, *et al.* BRAFV600E mutation is associated with preferential sensitivity to mitogen-activated protein kinase kinase inhibition in thyroid cancer cell lines. *The Journal of clinical endocrinology and metabolism* **2008**;93:2194-201
  34. Bejerano G, Pheasant M, Makunin I, Stephen S, Kent WJ, Mattick JS, *et al.* Ultraconserved elements in the human genome. *Science* **2004**;304:1321-5
  35. Xiong Y, Zhang L, Kebebew E. MiR-20a is upregulated in anaplastic thyroid cancer and targets LIMK1. *PloS one* **2014**;9:e96103
  36. Zhu H, Fang J, Zhang J, Zhao Z, Liu L, Wang J, *et al.* miR-182 targets CHL1 and controls tumor growth and invasion in papillary thyroid carcinoma. *Biochemical and biophysical research communications* **2014**;450:857-62
  37. Porreca I, De Felice E, Fagman H, Di Lauro R, Sordino P. Zebrafish bcl2l is a survival factor in thyroid development. *Developmental biology* **2012**;366:142-52
  38. Schweppe RE, Klopper JP, Korch C, Pugazhenti U, Benezra M, Knauf JA, *et al.* Deoxyribonucleic acid profiling analysis of 40 human thyroid cancer cell lines reveals cross-contamination resulting in cell line redundancy and misidentification. *The Journal of clinical endocrinology and metabolism* **2008**;93:4331-41
  39. Meireles AM, Preto A, Rocha AS, Rebocho AP, Maximo V, Pereira-Castro I, *et al.* Molecular and genotypic characterization of human thyroid follicular cell carcinoma-derived cell lines. *Thyroid : official journal of the American Thyroid Association* **2007**;17:707-15
  40. Rivera M, Sang C, Gerhard R, Ghossein R, Lin O. Anaplastic thyroid carcinoma: morphologic findings and PAX-8 expression in cytology specimens. *Acta cytologica* **2010**;54:668-72
  41. Becker N, Chernock RD, Nussenbaum B, Lewis JS, Jr. Prognostic significance of beta-human chorionic gonadotropin and PAX8 expression in anaplastic thyroid carcinoma. *Thyroid : official journal of the American Thyroid Association* **2014**;24:319-26
  42. Liu Y, Zhang B, Shi T, Qin H. miR-182 promotes tumor growth and increases chemoresistance of human anaplastic thyroid cancer by targeting tripartite motif 8. *OncoTargets and therapy* **2017**;10:1115-22
  43. Cabanillas ME, McFadden DG, Durante C. Thyroid cancer. *Lancet* **2016**;388:2783-95
  44. Fatica A, Bozzoni I. Long non-coding RNAs: new players in cell differentiation and development. *Nat Rev Genet* **2014**;15:7-21
  45. Flynn RA, Chang HY. Long noncoding RNAs in cell-fate programming and reprogramming. *Cell Stem Cell* **2014**;14:752-61
  46. Fuziwara CS, Kimura ET. MicroRNAs in thyroid development, function and tumorigenesis. *Molecular and cellular endocrinology* **2017**;456:44-50
  47. Peng X, Li W, Yuan L, Mehta RG, Kopelovich L, McCormick DL. Inhibition of proliferation and induction of autophagy by atorvastatin in PC3 prostate cancer cells correlate with downregulation of Bcl2 and upregulation of miR-182 and p21. *PloS one* **2013**;8:e70442

## Figure Legends

**Fig 1. *Klhl14-AS* is downregulated in thyroid cancer.** **A.** *Klhl14-AS* expression values of 12 PTC and their corresponding healthy samples reported as  $2^{-\Delta\text{Ct}}$  in scatter dot plot. The median with the interquartile range is shown. **B.** *Klhl14-AS* expression in ATC samples and in a pool of healthy thyroids (HT), reported as  $\text{Log}_{10}$  of the  $2^{-\Delta\Delta\text{Ct}}$  values. **C.** *Klhl14-AS* expression in thyroid cancer cell lines and wild type Nthy-ori 3-1, reported as  $2^{-\Delta\Delta\text{Ct}}$  values. **D.** *Klhl14-AS* levels in ER<sup>TM</sup>RAS<sup>V12</sup>FRTL-5 treated for 24 hours with vehicle (NT) or Tamoxifene (+4OHT) to induce Ras oncogenic activation. **E.** *Klhl14-AS* levels in parental FRTL-5 cells and H-RAS<sup>V12</sup>FRTL-5. Data in D and E are shown as  $\text{Log}_{10}$  of the  $2^{-\Delta\Delta\text{Ct}}$  values. **F.** *Klhl14-AS* expression analyzed by in situ hybridization in Tg-rtTA-TetO-BrafV600E mouse thyroids. Mice were treated with doxycycline (+DOX) or left untreated (NT). 200x and 1000x magnifications are shown. **G.** *Klhl14-AS* was measured on pools of untreated (NT) and treated (+DOX) thyroids. All data are shown as means  $\pm$  SD. \*  $p < 0.05$ ; \*\*  $p < 0.01$ ; \*\*\*  $p < 0.001$ .

**Fig 2. *Klhl14-AS* knockdown affects thyroid cells differentiation and viability.** **A.** *Klhl14-AS* was knocked-down in FRTL-5 using specific LNA Gapmers (*Khl14-AS* LNA) or control LNA (ctr LNA). Thyroid differentiation markers levels were evaluated through qRT-PCR. For each gene, value obtained in ctr LNA-transfected cells was set at 1 (dotted line). **B.** Control and *Klhl14-AS* knocked-down FRTL-5 were counted upon Trypan blue staining. The number of viable and dead cells is expressed as percentage of the total counted cells. **C.** MTS assay performed on the samples shown in B. Absorbance values on the graph represent the average of four replicates. **D.** Ki67 positive nuclei percentage of control and *Klhl14-AS* knocked-down FRTL-5. **E.** Ki67 immunofluorescence of control and *Klhl14-AS* knocked-down FRTL-5. Scale bar represents 50 $\mu\text{m}$ . **F.** *KLHL14-AS* was knocked-down in Nthy-ori 3-1 using specific LNA Gapmers (*KLHL14-AS* LNA) or control LNA (ctr LNA). Thyroid differentiation markers evaluation was performed as in A. **G.** Control and *Klhl14-AS* knocked-down Nthy-ori 3-1 were counted upon Trypan blue staining. The number of viable and dead cells is expressed as percentage of the total counted cells. **H.** MTS assays performed on the samples shown in G. Absorbance values on the graph represent the average of four replicates. The data are representative of three independent experiments. All data are shown as means  $\pm$  SD. \*  $p < 0.05$ ; \*\*  $p < 0.01$ ; \*\*\*  $p < 0.001$ .

**Fig 3. *Klhl14-AS* is target of miR-182-5p and miR-20a-5p.** **A.** Luciferase activity of pGL3control vector containing *Klhl14-AS* highly conserved region (HCR) or its antisense sequence (HCR AS) co-transfected with control (miR-ctr) or specific miRNA (*Mir182-5p* and *Mir20a-5p*) mimics. **B.** Endogenous *Klhl14-AS* levels in FRTL5 transfected with control, *Mir182-5p* and *Mir20a-5p* mimics. **C.** *Klhl14-AS* expression in TPC1 and BCPAP transfected with control (neg.ctr LNA) or specific miRNA inhibitors (*MIR182-5p* LNA and *MIR20a-5p* LNA). **D.** TPC1 cells transfected as in C were counted upon Trypan blue staining. The number of viable and dead cells is expressed as percentage of the total counted cells. **E.** MTS assays performed on the samples shown in D. Absorbance values on the

graph represent the average of four replicates. **F.** *Klhl14-AS* pull-down performed in FRTL-5 with antisense DNA oligonucleotides complementary to *Klhl14-AS*. Beads conjugated with LacZ oligonucleotides (LacZ) or unconjugated beads (BO) were used as controls. Recovered *Klhl14-AS* from input and pulled-down extracts was measured by qRT-PCR. **G.** Western blot analysis of AGO2 and ACTIN from input and pulled-down extracts. **H.** *Mir182-5p* recovery indicated as the percentage of the input. **I.** *Mir20a-5p* recovery shown as in F. Input represents 10% of the extract used for the pull-down. The data are representative of three independent experiments. All data are shown as means  $\pm$  SD. \*  $p < 0.05$ ; \*\*  $p < 0.01$ ; \*\*\*  $p < 0.001$ .

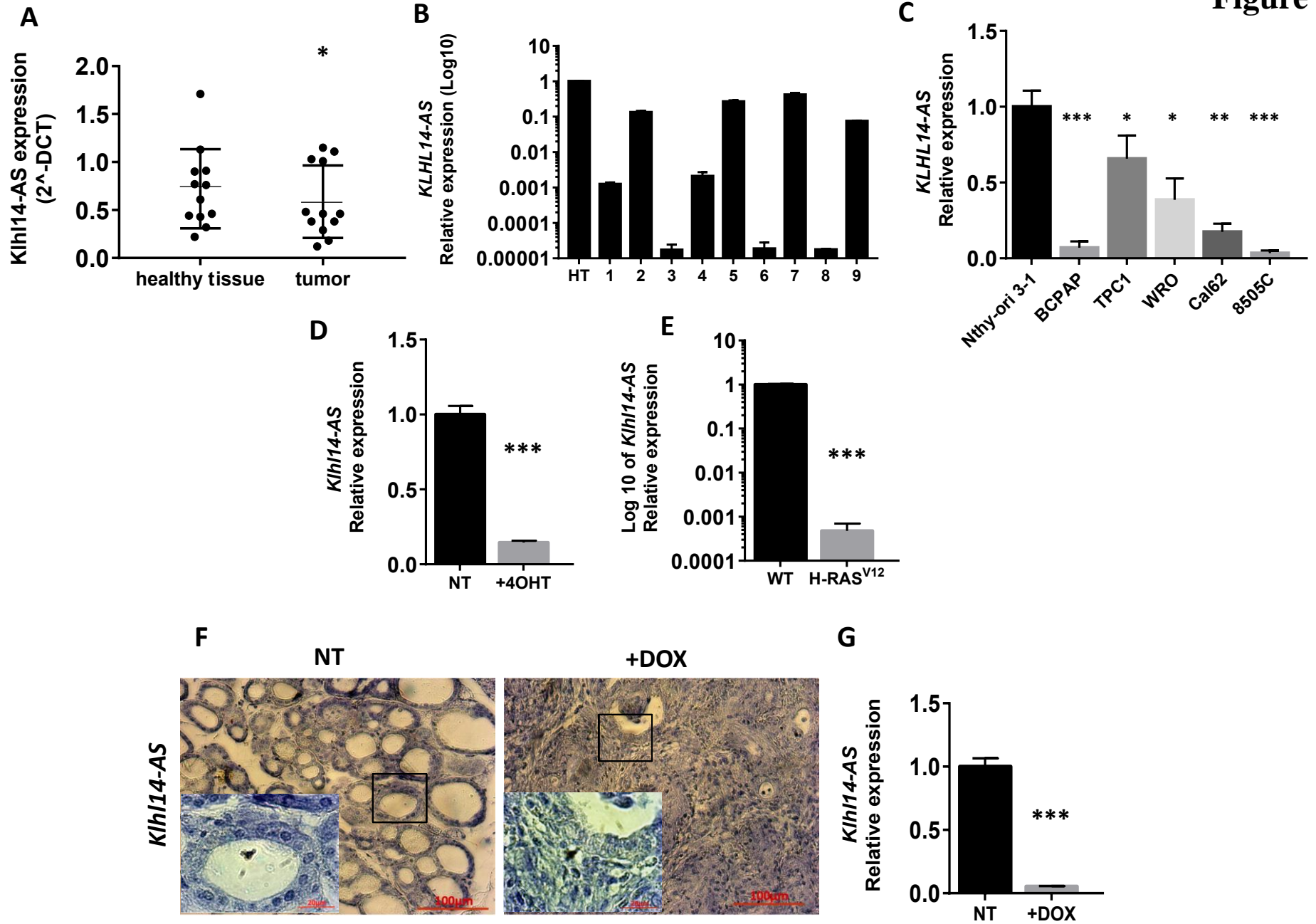
**Fig 4. Validation of *Pax8* and *Bcl2* as miRNAs targets.** **A.** Endogenous levels of *Pax8* and *Bcl2* transcripts in FRTL-5 evaluated after control (miR-ctr), *Mir182-5p* and *Mir20a-5p* mimics transfection by qRT-PCR. **B.** Western blot analysis of PAX8 and BCL-2 of samples transfected as in A (left panel) and the respective densitometric analysis (right panel). **C.** Luciferase activity of pGL3control vector containing MRE-containing region (MCR) of rat *Pax8* transcript or its antisense sequence (MCR AS) co-transfected with control (miR-ctr) or specific miRNA (*Mir182-5p* and *Mir20a-5p*) mimics. **D.** Luciferase activity of pGL3 control vector containing MCR of rat *Bcl2* transcript or its antisense sequence (MCR AS) co-transfected with control (miR-ctr) or specific *Mir182-5p* mimic. The data are representative of three independent experiments. All data are shown as means  $\pm$  SD. \*  $p < 0.05$ ; \*\*  $p < 0.01$ ; \*\*\*  $p < 0.001$ .

**Fig 5. *Klhl14-AS* regulates *Pax8* and *Bcl2* acting as a miRNAs decoy.** **A.** *Bcl2* expression in ER<sup>TM</sup>RAS<sup>V12</sup>FRTL-5 treated for 24 hours with vehicle (NT) or Tamoxifene (+4OHT) to induce Ras oncogenic activation. **B.** *Bcl2* levels in parental FRTL-5 and H-RAS<sup>V12</sup>FRTL-5. **C.** *Bcl2* in Tg-rtTA-TetO-BrafV600E mouse thyroids. Mice were treated with doxycycline to induce thyroid cancer (+DOX) or left untreated (NT). **D.** *Bcl2* expression levels in thyroid cancer and normal human cell lines. **E.** *Bcl2* expression in control (ctr LNA) and *Klhl14-AS* LNA transfected FRTL-5 and Nthy-ori 3-1. **F.** *Pax8* and *Bcl2* expression in FRTL-5 transfected with control or *Klhl14-AS* LNA together with control or Dicer specific siRNA (ctr siRNA and Dicer siRNA). Data are shown as fold change of ctrLNA+ctrsiRNA sample. **G.** *Pax8* and *Bcl2* expression in FRTL-5 transfected with *Mir182-5p* or *Mir20a-5p* mimics together with pCEFL*Klhl14-AS* or empty vector (ev). **H.** Thyroid differentiation markers expression in control and *Klhl14-AS* silenced FRTL-5 treated with Actinomycin D (Acto-D). **I.** Thyroid differentiation markers expression in FRTL-5 transfected with control (ctr LNA) and *Klhl14-AS* LNA, in combination with pCEFL*Pax8*, pCEFL*Bcl2* or empty vector. Primers used for *Pax8* and *Bcl2* do not amplify ectopic mRNAs being designed on UTR of both genes. Data are shown as fold change of ctrLNA+ev sample. All data in the figure are obtained through qRT-PCR and are shown as means  $\pm$  SD. \*  $p < 0.05$ ; \*\*  $p < 0.01$ ; \*\*\*  $p < 0.001$ .

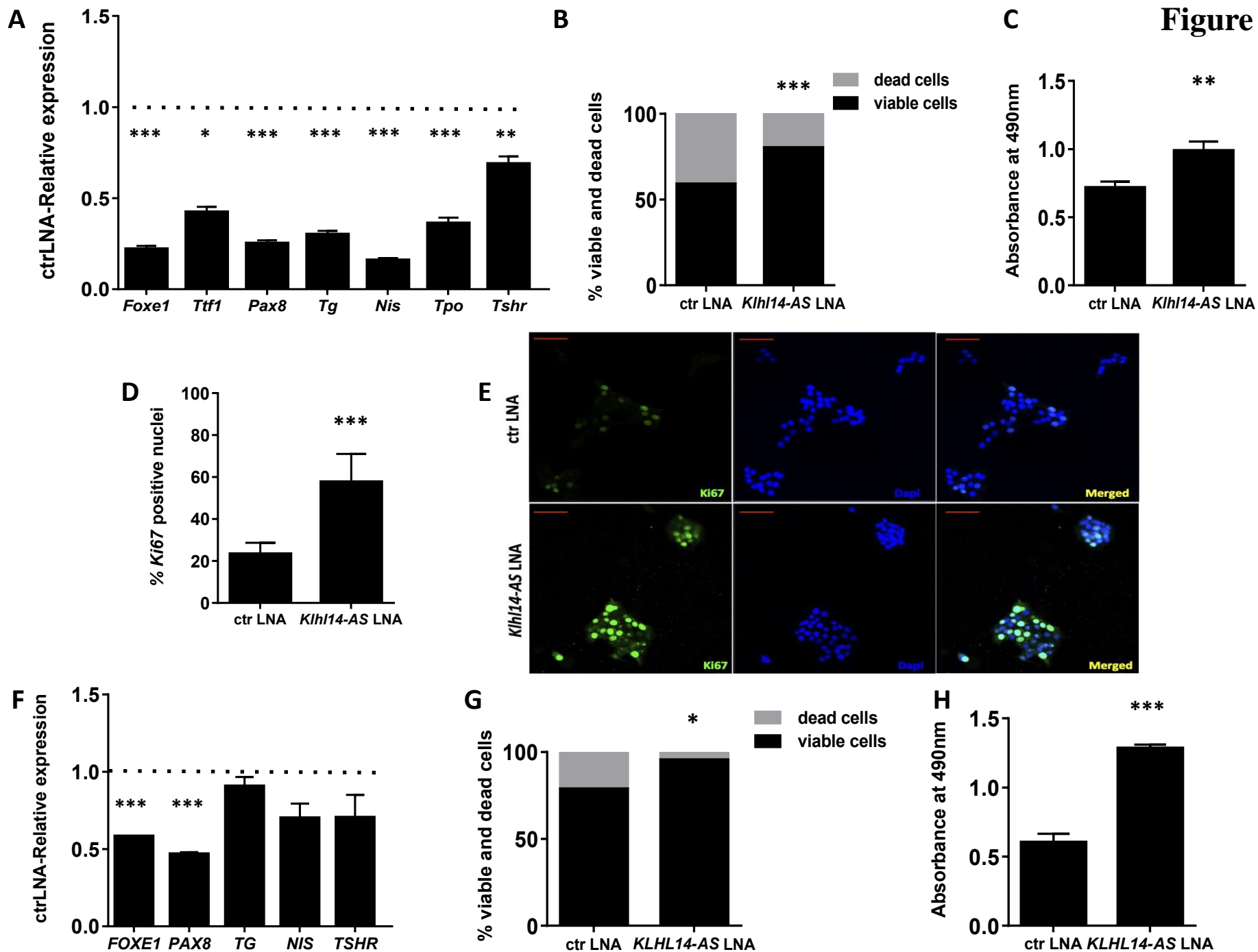
**Fig 6. *Pax8* and *Bcl2* expression positively correlates with that of *Klhl14-AS* in human thyroid cancer.** **A.** Relative expression of *Pax8* and *Bcl2* in ATC samples and in a pool of healthy thyroids (HT). Data are shown as means  $\pm$  SD. **B.** *Pax8* expression values in 12 PTC and their corresponding healthy samples reported as  $2^{-\Delta\Delta Ct}$  in scatter dot plot. The median with the interquartile range is shown. **C.** *Bcl2* expression measured as described for *Pax8* in B. **D.** Correlation analysis of *Klhl14-AS*

and *Pax8* expression values in the 12 PTC samples analyzed. Pearson's correlation coefficient tests were performed using GraphPad Software. **E.** Correlation analysis of *Klhl14-AS* and *Bcl2* expression values in the 12 PTC samples analyzed as described for *Pax8* in D. Data are obtained through qRT-PCR and are shown as means  $\pm$  SD. \*  $p < 0.05$ ; \*\*  $p < 0.01$ ; \*\*\*  $p < 0.001$ .

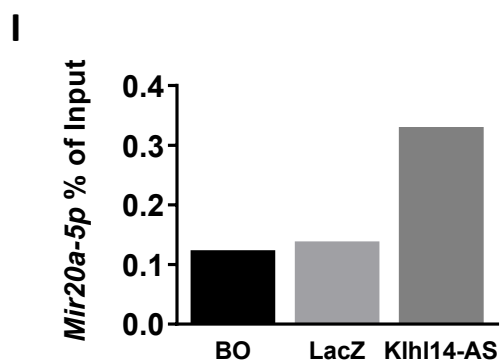
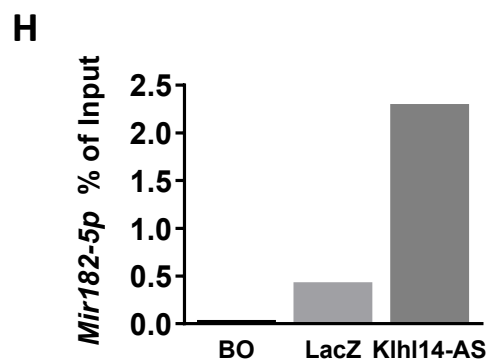
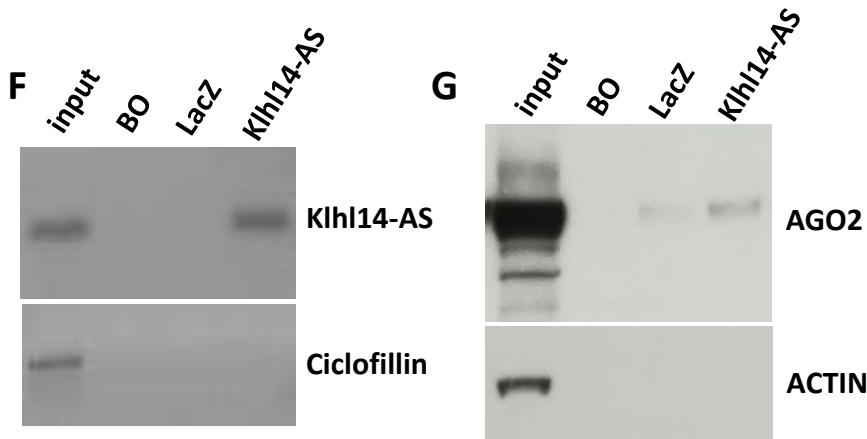
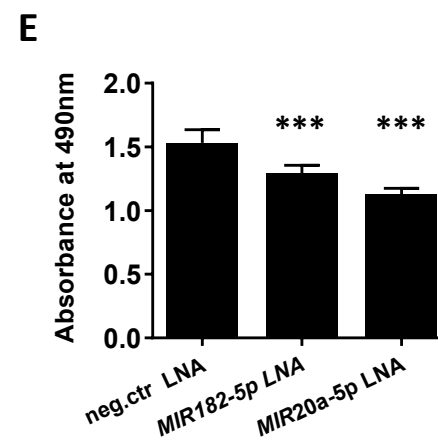
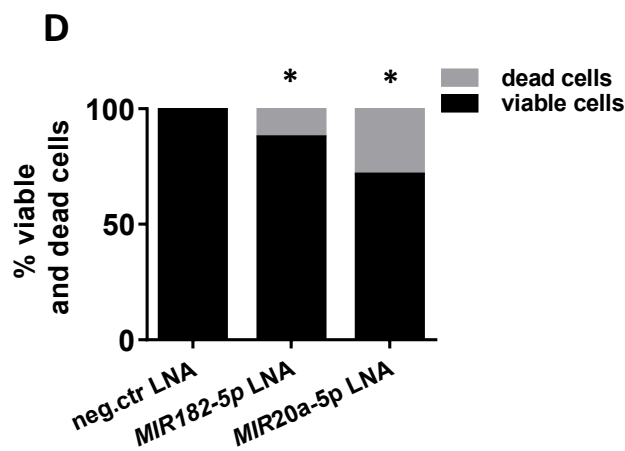
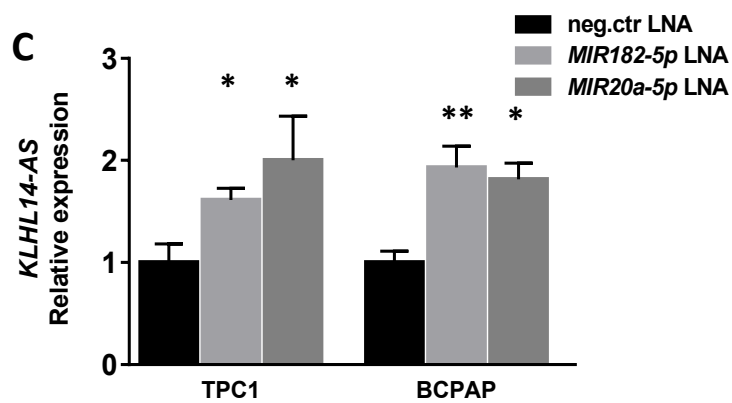
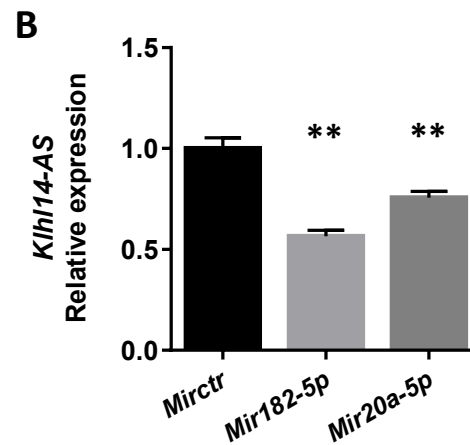
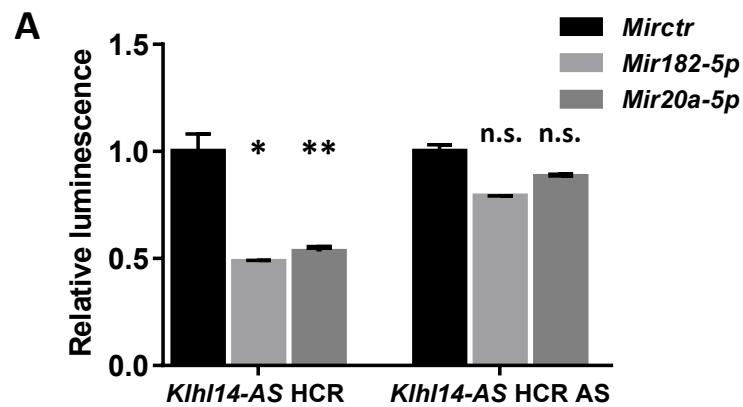
**Fig 7. *MIR182-5p* and *MIR20a-5p* are upregulated in thyroid cancer.** **A.** *MIR182-5p* expression values in 6 PTC and their corresponding healthy samples reported as  $2^{-\Delta Ct}$  in scatter dot plot. The median with the interquartile range is shown. **B.** *MIR20a-5p* expression values were analysed as in A. **C.** *MIR182-5p* and *MIR20a-5p* expression in ATC samples and in a pool of healthy thyroid tissues, arbitrarily set as 1 (dotted line). **D.** Relative expression of *MIR182-5p* and *MIR20a-5p* in thyroid cancer cell lines. The expression was compared to that measured in a pool of healthy thyroid tissues, arbitrarily set as 1. The data are shown as Log10 of the  $2^{-\Delta\Delta Ct}$  values. **E.** *Mir182-5p* and *Mir20a-5p* levels in parental FRTL-5 and H-RAS<sup>V12</sup>FRTL-5. **F.** *Mir182-5p* and *Mir20a-5p* expression in thyroids from Tg-rtTA-TetO-BrafV600E mice treated with doxycycline (+DOX) or left untreated (NT). All data are obtained through qRT-PCR are shown as means  $\pm$  SD. \*  $p < 0.05$ ; \*\*  $p < 0.01$ ; \*\*\*  $p < 0.001$ .

**Figure 1**

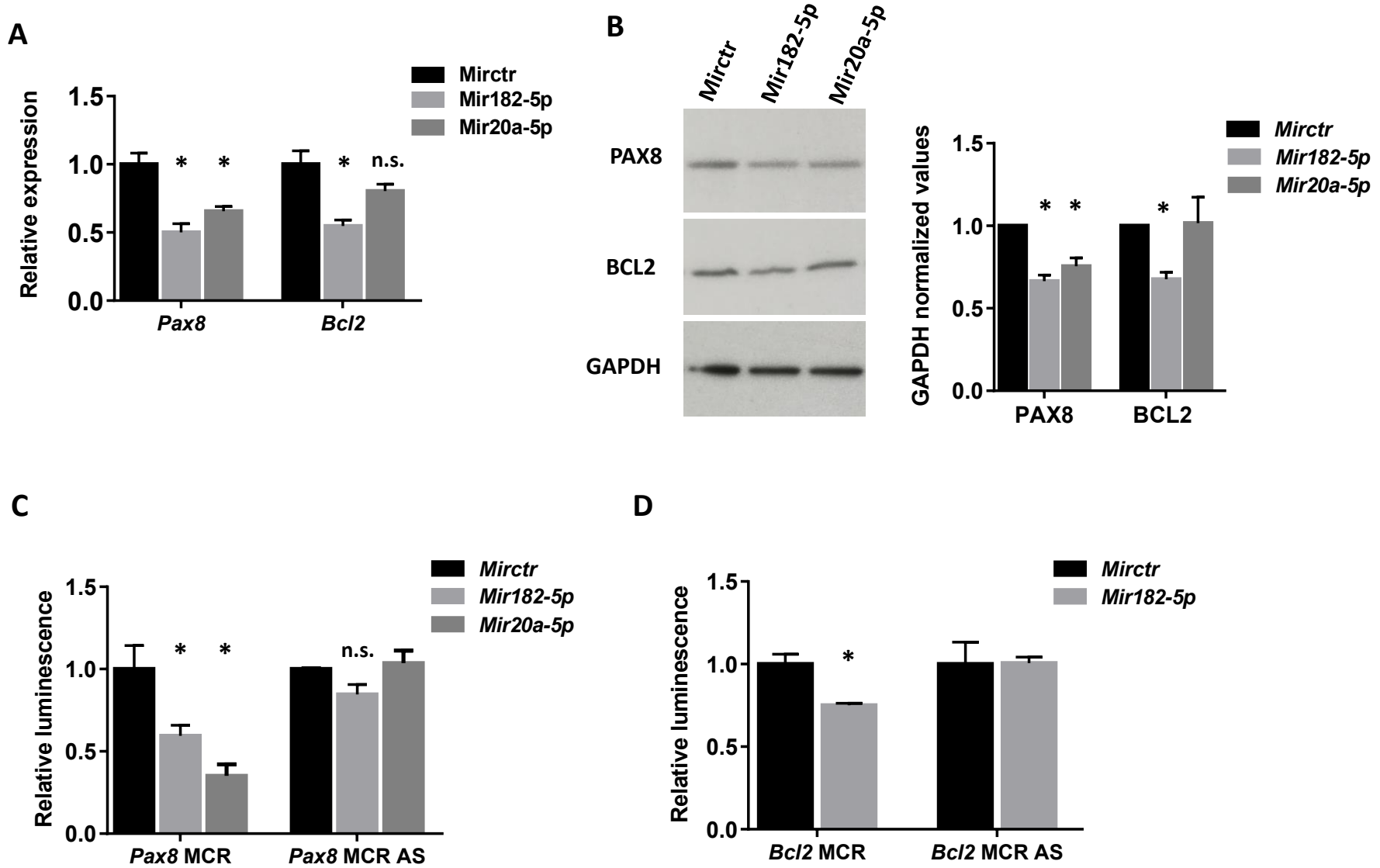
**Figure 2**

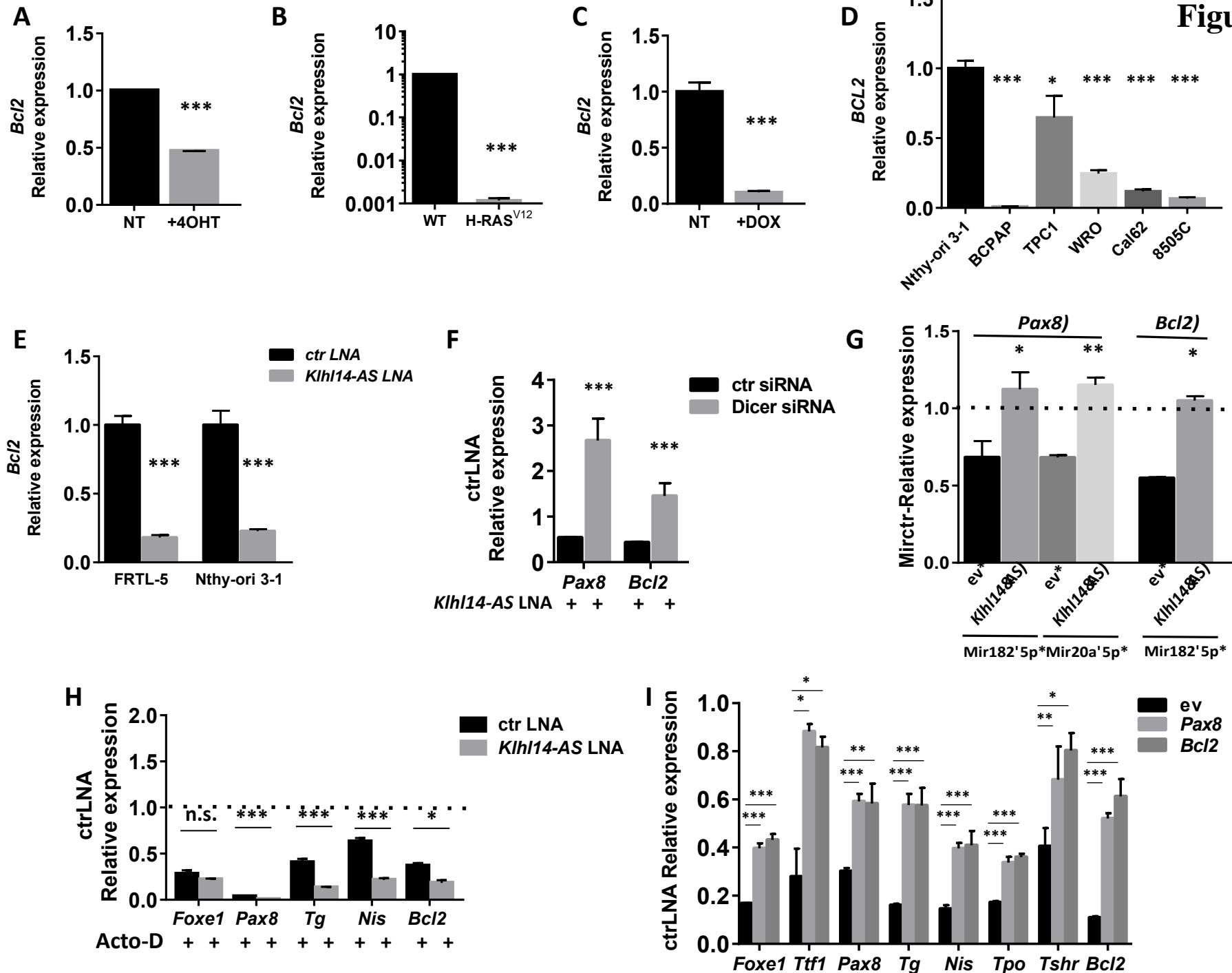


**Figure 3**



**Figure 4**





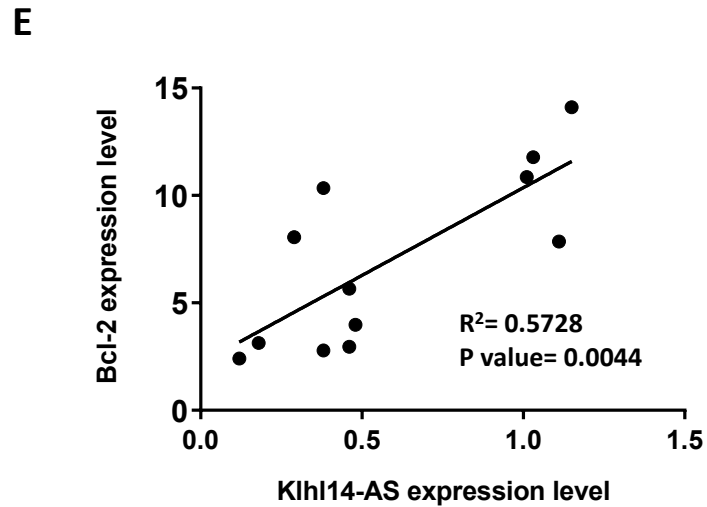
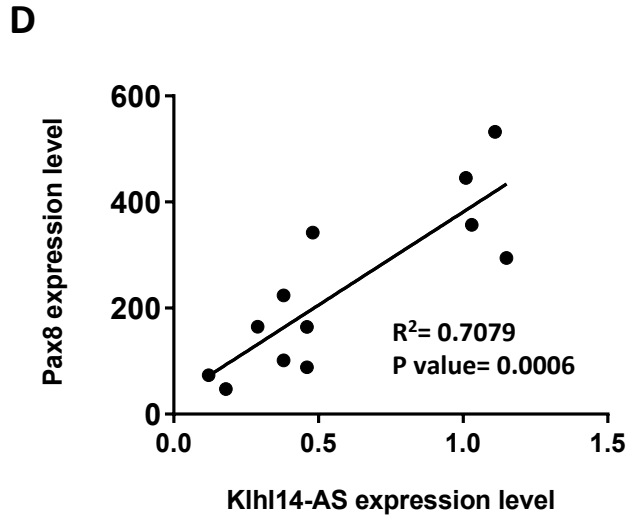
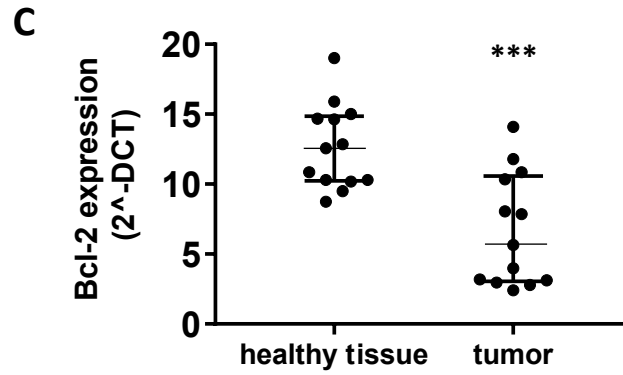
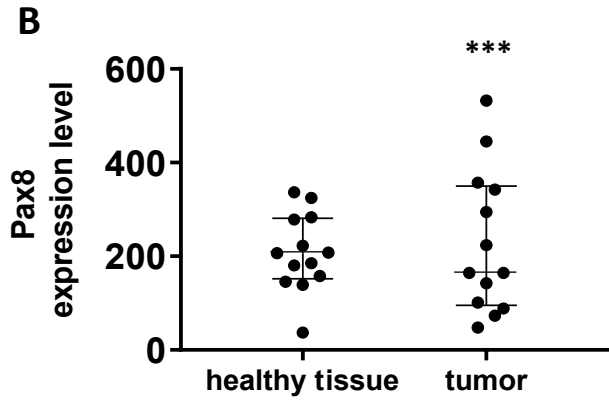
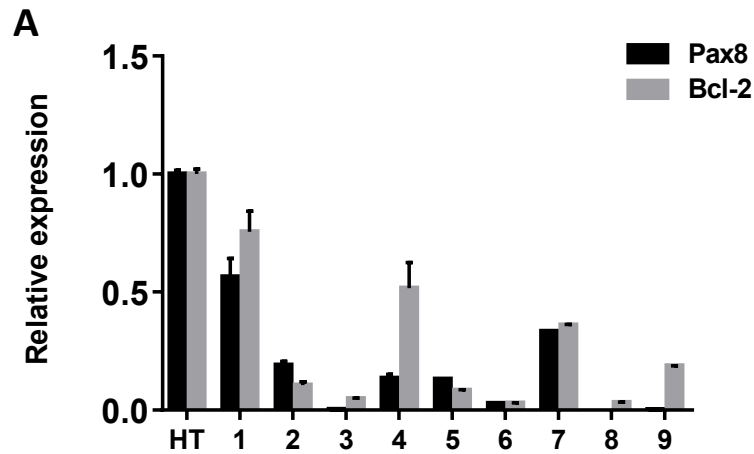


Figure 7

